Electro-rotation and electro-translation of colloidal particles in liquid crystals

G. Liao, I. I. Smalyukh, J. R. Kelly, O.D. Lavrentovich, A. Jákli

Liquid Crystal Institute and Chemical Physics Interdisciplinary Program, Kent State University
Kent, OH 44242, USA

Abstract

We present the first observations of DC electric-field-induced rotational and translational motion of finite particles in liquid crystals. We show that the electro-rotation is essentially identical to the well - known Quincke rotation, which in liquid crystals triggers an additional translational motion at higher fields. In the smectic phase the translational motion is confined to the two-dimensional geometry of smectic layers, in contrast to the isotropic and nematic phases, where the particles can move in all three dimensions. We demonstrate that by proper analysis of the electro-rotation one can determine the in plane viscosity of smectic liquid crystals. This method needs only a small amount of material, does not require uniform alignment over large areas, and allows one to probe rheological properties locally.

Introduction

Electrophoresis, i.e. electrically-induced rotational and translational motion of small particles in fluids, is an ancient, but still active science.[1] Most electrophoretic motions are allowed by symmetry (e.g. along the field), however some motions require symmetry breaking transitions, and appear only above a threshold electric field. An example of the latter is a DC electric-field-induced steady rotation of solid spherical objects that, in isotropic liquids, was observed first in 1893 by Weiler[2] (Quincke rotation[3]), but was explained only in 1984 by Jones[4]. Another interesting example is an induced translational motion normal to the electric field. This has been observed only for long, slender particles whose charges vary along their contour[5] and was explained in terms of coupling between surface charge and shape modulation.[6] Electrophoretic studies in liquid crystals are scarce[7] and are limited to motions of nanoparticles in lyotropic liquid crystals that do not require symmetry breaking transitions. It is clear, however, that the techniques based on one-bead microrheology[8] developed recently to monitor the mechanical properties of viscoelastic soft materials[9], might be extremely helpful in analyzing rheological properties of smectic liquid crystal materials, which can be considered as stacks of two-dimensional fluid layers. The experimental verification of the two - dimensional fluid nature of the smectic phases by traditional macro-rheology[10,11] however is very difficult due to generation of defects by the macroscopic flow.[12,13] In this letter we report the first observations of electro-rotation and electro-translation of microscopic cylindrical and spherical inclusions dispersed in smectic materials. We show that quantitative analysis of the electro-rotation can be used to determine the in plane viscosity of the smectic liquid crystals.

Results

We have studied two commercially available liquid crystalline (*LC*) materials: octyl cyano biphenyl (8CB) from Aldrich, and a mixture CS 2003 from Chisso, Inc. 8CB has a smectic A (SmA) phase in temperature range 23 - 33^{o}C characterized by a large positive dielectric anisotropy ($\Delta\varepsilon$=8 at 32^{o}C). CS2003 is a room temperature ferroelectric SmC* mixture with ferroelectric polarization P_o~40nC/cm^2 and negative dielectric anisotropy ($\Delta\varepsilon$=-0.6 at 50^{o}C). It

http://www.e-lc.org/docs/2005_02_25_10_57_49

also has a SmA* phase between 56°C and 64°C, and a chiral nematic (N*) phase between 64°C and 90°C. For Fluorescence Confocal Polarizing Microscopy (FCPM) observations the LCs were doped with ~0.01 % of fluorescent dye BTBP (N,N'-Bis(2,5-di-tert-butylphenyl)-3,4,9,10-perylenedicarboximide).[14] Glass spheres (beads) of 4.5μm diameter and cylinders of 4.5μm and 10μm diameters with length/diameter ratios varying between 1 and 10, were dispersed at low concentrations in LC films of thicknesses in the range of 6-30μm. The observations were carried out by polarizing microscopy (Olympus BX60), and by a fast version of FCPM based on a scanning CARV® system with a spinning Nipkow disk integrated with a Nikon microscope (Eclipse E-600) that enabled taking motion pictures of the textures. The electric field was applied normal to the film surfaces via a potential difference between transparent indium tin oxide (ITO) layers deposited on the glass plates of the cells. The ITO layers were coated with a polyimide (PI2555 from HD Micro Systems) film rubbed uni-directionally to promote director alignment parallel to the rubbing direction.

Far from the dispersed particles such a surface treatment produced uniform bookshelf layer structure (layers are normal to the substrates). In case of CS2003 ($\Delta\varepsilon<0$) this alignment remained stable in electric fields applied across the substrates. In case of 8CB ($\Delta\varepsilon>0$), a sufficiently strong field realigns the layers from their original bookshelf vertical orientation. In the transition range (2.5V/μm < E < 4V/μm) the layers are tilted with numerous defects. At *E>4V/μm* a fairly uniform homeotropic configuration forms, i.e. the smectic layers are parallel to the substrates. If the field is switched off, the resulting texture depends on the pre-applied field: if it is smaller than *7V/μm*, the bookshelf structure gradually restores itself; however, if the field is larger than *7V/μm*, the surface anchoring is broken, the homeotropic texture is preserved at zero electric field as a metastable state.

In the bookshelf textures at zero electric fields, most of the *glass cylinders* are aligned parallel to the rubbing direction, i.e., along the director. FCPM textures of the vertical cross-sections of the 8CB samples, *Figure 1* (a), show that the director is parallel to the cylinder surface everywhere; two toric focal conic domains[15] cup the ends of the cylinder.

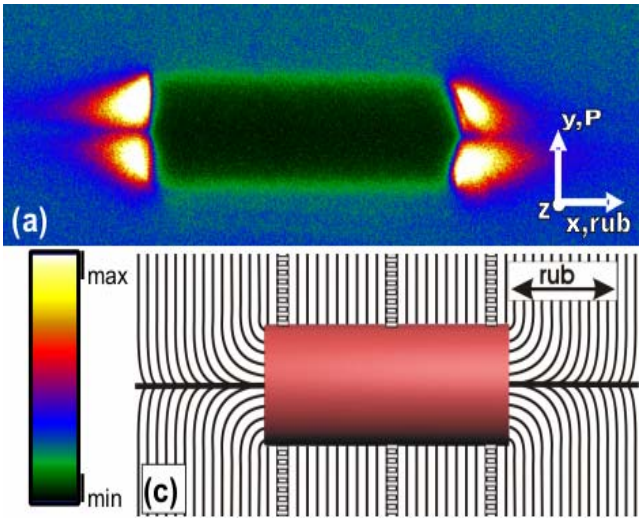

Figure 1: (a): In plane FCPM texture of a 4.5μm cylinder; (b): The FCPM color coded intensity scale; (c): The reconstructed director and layer structure that has rotational symmetry with respect to the cylinder axis.

http://www.e-lc.org/docs/2005_02_25_10_57_49

When the DC field exceeds the threshold E_r, the cylinders start to rotate about their symmetry axes. The rotation of the cylinders is easily observable under the microscope, as the edges of the cylinders are often slanted. Both the threshold field, E_r, and the angular frequency of rotation, $\omega(E)$, could be measured by recording the rotation and tracking the frames. The electric field dependence of the angular velocity for CS2003 at 59°C (SmA phase) and at 50°C (SmC* phase) are plotted in Figure 2/a. The threshold E_r was observed rapidly increasing at decreasing temperatures (0.34V/μm at 59°C and 2.1V/μm at 50°C), however the slope of the curves at field much higher than the threshold only slightly depend on the temperature. The determination of the threshold is not precise (~10% error), because the onset varies slightly from particle to particle, and some of the particles oscillates back and forth near the threshold. Within the measurement error cylinders with different radii rotate with the same angular velocity. The rotation velocity is basically independent of the length of the cylinders if the length/ diameter ratio is larger than about 5. Shallow cylinders rotate significantly slower, because the defects near the edges become more important.

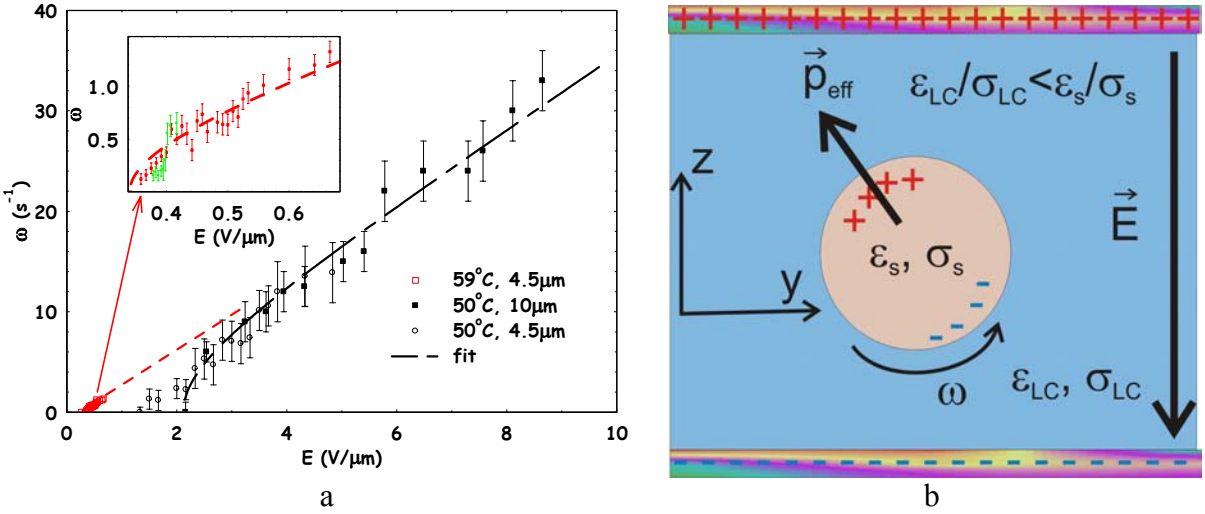

Figure 2: (a) The measured electric field dependence of the angular frequency of 4.5μm and 10μm diameter cylinders embedded in 12μm thick CS2003 sample at 50°C and 59°C . Dashed lines are fits using Eq. (4) with viscosities η=5.5Pas and η=0.9Pas, respectively. (b) Illustration of the proposed physical mechanism[4] leading to the electro-rotation.

Similar angular velocity values could be measured at around 3 times smaller fields in 8CB at 32°C (for example at 2.5V/μm ω~30s^{-1}), although there, the data scatter much more due to the field - induced layer realignment.

Electro-rotations with lower thresholds were observed in the nematic, and in the isotropic phases of both materials, indicating that the effect does not require anisotropy, similar to the classical Quincke rotation[3], which only require that the charge relaxation time of the inclusion ($\tau_s = \varepsilon_s / \sigma_s$) be larger than the charge relaxation time of the liquid matrix ($\tau_l = \varepsilon_l / \sigma_l$). This is easily satisfied for liquid crystals ($\tau_s > \tau_{lc}$), because the conductivity of the glass particles ($\sigma_s < 10^{-12}$Sm^{-1}) is much smaller than that of the liquid crystals (σ_{lc}=0.9x10^{-9}S/m for CS2003, and σ_{lc}~0.7x10^{-9} S/m for 8CB), whereas the relative dielectric constants are comparable (ε_s=3.9, $\varepsilon_{\parallel}(8CB) = 14$, $\varepsilon_{\perp}(8CB) = 6$, $\varepsilon_{\parallel}(CS2003) = 3$, $\varepsilon_{\perp}(CS2003) = 3.6$). In such a case, the distribution of free charges on the inclusion's surface is such that they are repelled from the

electrodes (i.e., the negative charge on the cylindrical surface is close to the negative electrode, Figure 2/b). This situation is unstable against small rotational perturbations, and the solid inclusion will rotate around the axis perpendicular to the applied field, as observed in the experiment. Although the theoretical description of the Quincke rotation for the case of spheres in isotropic fluids cannot be directly adopted for describing cylinders rotating in the liquid crystals, the underlying physics is similar. Neglecting edge effects, the rotation of slender cylinders involves a two dimensional flow; consequently we need a 2-D model. Such a model was worked out by Feng[16] and provides formula for the threshold electric field E_r, given as:

$$E_r^2 = \alpha \cdot \eta \left[(1+S)(1+R) \right] / \left[\varepsilon_l (1 - \tau_l / \tau_s) \tau_{MW} \right] \quad (1)$$

This expression is valid both for spheres and slender cylinders, only the parameters are different. For spheres[17] $\alpha = 4/3$, $S = \frac{2\varepsilon_l}{\varepsilon_s}$, $R = \frac{\sigma_s}{2\sigma_l}$ and $\tau_{MW} = (\varepsilon_s + 2\varepsilon_l)/(\sigma_s + 2\sigma_l)$, whereas for slender cylinders[16] $\alpha = 1$, $S = \frac{\varepsilon_l}{\varepsilon_s}$, $R = \frac{\sigma_s}{\sigma_l}$ and $\tau_{MW} = (\varepsilon_s + \varepsilon_l)/(\sigma_s + \sigma_l)$. In these expressions ε_l, σ_l (ε_s, σ_s) are the dielectric constant and electrical conductivity of the liquid (solid), respectively, τ_{MW} is the Maxwell-Wagner interfacial polarization relaxation time, and η is the viscosity.

For both spheres and cylinders the angular velocity as a function of the applied field can be given as

$$\omega = \frac{1}{\tau_{MW}} \sqrt{\frac{E^2}{E_r^2} - 1} \quad (2)$$

In case of our slender cylinder – liquid crystal system, where $\sigma_{lc} >> \sigma_s$ and $\varepsilon_{lc} \sim \varepsilon_s$, the expression for the threshold electric field simplifies to

$$E_r^2 \simeq \eta \frac{\sigma_{lc}}{\varepsilon_o^2 \varepsilon_{lc} \varepsilon_s} \quad (3)$$

where the relevant viscosity corresponds to the Miesovitz component η_a, because the shear plane is perpendicular to the director. [10] From the measured threshold field, additional electrical conductivity and the dielectric constants data one can get the viscosity from Eq.(3). With the parameters of *CS2003* at 50°C listed above, we get η=6 Pas, whereas in case of 8CB at 32°C we obtain only $\eta \sim 1$ Pas.

Actually, we can determine the viscosity even without the need of measuring the conductivity and the dielectric constant of the LC, by measuring both E_r and ω, and combining Eq.(2) and (3), giving

$$\omega(E) = \frac{E_r^2 \varepsilon_s \varepsilon_o}{\eta (1 + \varepsilon_s / \varepsilon_{lc})} \sqrt{\frac{E^2}{E_r^2} - 1}, \quad (4)$$

http://www.e-lc.org/docs/2005_02_25_10_57_49

For $E>>E_r$ this further simplifies to $\omega(E)=\frac{E_r\varepsilon_s\varepsilon_o E}{\eta\left(1+\varepsilon_s/\varepsilon_{lc}\right)}$. In spite of the ambiguity in determining the angular velocity near the threshold, the electric field dependence of the measured angular frequency can be satisfactorily fitted by Eq.(4) (see *Figure 1*(e) for CS2003 at 50°C and 59°C), giving η_a *=5.5Pas and* η_a*=0.9Pas,* at 50°C and 59°C, respectively. Electro-rotation measurements for 8CB at 32°C gave E_r*=0.6V/μm* and $\omega(E \gg E_r)/E \sim 12\cdot 10^{-6}\, mV^{-1}s^{-1}$ which provide η_a *=1.6Pas*. These values are in fairly good agreement with the results obtained using conductivity and dielectric data, and only the threshold field measurement. We note that η_a was already measured for 8CB and it was found[18] to be ~1.5Pas at shear rates corresponding to the highest rates ($50s^{-1}$) in our experiments. This agreement clearly indicates that electro-rotation of cylindrical inclusions can be used to study the rheology of liquid crystals.

At further increasing fields ($E>E_{th}$), the rotating cylinders are set into translational motion, too. In the isotropic and nematic phases the direction of the motion occurs in three dimensions; however, in the smectic phases the axes of the cylinders move strictly along the smectic layers, i.e., the motion is two-dimensional. Due to the irregular shape of the edges of the cylinders the speed of the motion is somewhat irregular. To obtain more reliable results from the field-induced translational motion we studied spherical beads instead of cylinders.

At zero electric fields in the bookshelf smectic layer alignment, the *spherical beads* are surrounded by two defect "wings" spanning along the layer normal (Figure 3), similar to defect lines around isotropic droplets in SmA liquid crystals of planar anchoring reported by Blanc and Kleman.[19] The length of the wings is about 30-100μm in the SmA phases of both 8CB and CS2003, whereas in the SmC* structure the wings are much shorter (~5-10μm), and sometimes are not even observable.

Although their electro-rotation cannot be easily seen (they are too symmetric), careful observations revealed that they also spin around their axes normal to the field before they begin to translate. Similar to the cylinders, the translational motions occur above threshold electric fields $E_{th}>E_r$ (E_{th}~3.5V/μm for CS2003 at T=50°C and E_{th}~2.5V/μm for 8CB at T=32°C). The translational motion takes place along the smectic layers. One obvious explanation of this translation is that there is a horizontal gradient of the electric field. Since the dielectric constant of the particles is smaller than of the liquid crystal, this would result in a net force pulling the bead toward the smaller fields. To check this we made wedge cells up to the wedge angle of $2\cdot 10^{-3}\, rad$, but we did not find measurable difference in the direction of the translation with respect to the direction of the gradient of the film thickness. This may not be surprising, since the local (in the range of 50-100μm) film thickness variation may be an order of magnitude larger than the wedge angle. In fact, because the electro-translation occurs above the threshold of the electro-rotation, the source for the local field gradient may be the electro-rotation itself. The spinning of the particles may result in an asymmetric charge distribution around the inclusions leading to an imbalance in the magnitude of the vertical electric fields, which may result in a local field gradient much larger than due to film thickness variation.

FCPM studies show that at zero fields the beads are evenly distributed between the substrates, but when the translational motion is induced, they eventually all end up at either the top or bottom of the film (Figure 3/d-g), where they move along the substrates. When the fields are turned off the beads stick to the substrates and do not move back toward inside of the film.

http://www.e-lc.org/docs/2005_02_25_10_57_49

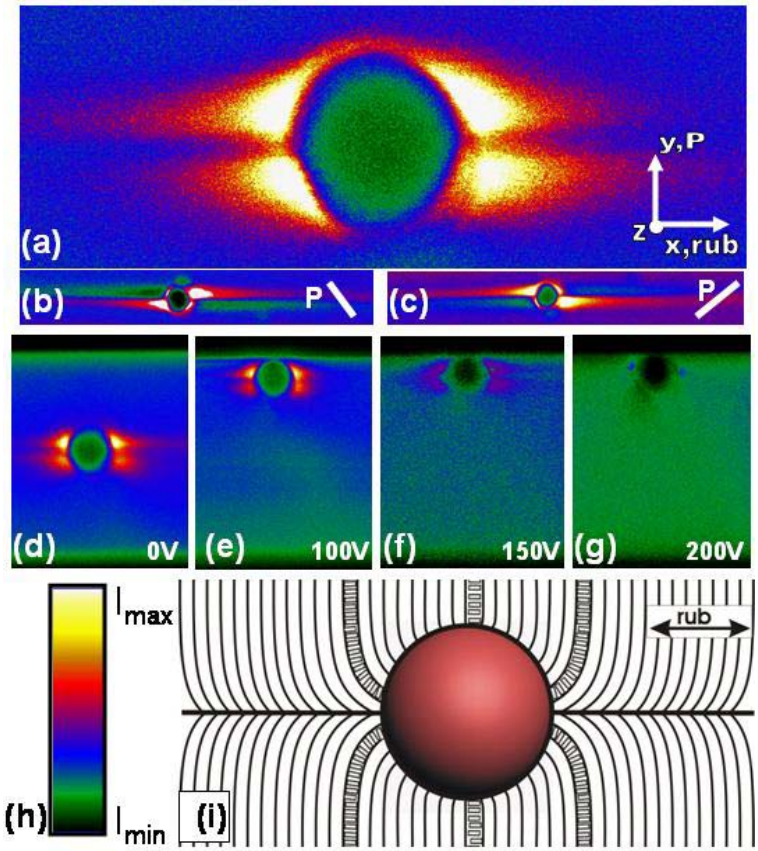

Figure 3: In-plane FCPM texture of the director distortions of 8CB at room temperature around a 4.5μm spherical particle. (a-d:) Far from the beads the liquid crystal is in bookshelf geometry (layers normal to substrates). A linear polarizer is orthogonal (a) and at about ±45°(b,c) to the rubbing direction; (d): Vertical FCPM cross-section with the particle at rest close to the center of a 30μm thick cell at zero field. Note that the director distortions at the particle are similar to those in the in-plane section, indicating rotational symmetry around the defect line; (e-g): Vertical FCPM cross-sections indicating changes of particle positions and distortions in director field around the spheres at different electric fields. The layers are distorted in (e,f) and practically parallel to the substrates in (g); (h): The FCPM color-coded intensity scale; (i):Reconstructed layers and director pattern around the particle embedded in the system of parallel smectic layers.

The electric field dependence of the translational motion was characterized by measuring the maximum distance (s_m) the beads traveled along the substrates during one-second-long voltage pulses, and s_f, which is the final distance the beads were found from the starting point long after the pulse was switched off. In the *SmA* phase of the studied materials there is a narrow range above E_{th} where the particles travel by less than their diameter and bounce back after the field is turned off ($s_f \sim 0$). This indicates elastic behavior, which is due to the layer distortions around the particles (see Figure 3/i). At higher fields the particles travel much further than their diameter and only partially recoil after the field removal. This is characterized by the parameter $\Gamma = s_f / s_m < 1$ and indicates viscoelastic behavior. In this range the defect wings shrink and gradually vanish (Figure 3(e-g)). At fields higher than E_v (~7V/μm for 8CB at T=32°C and ~6V/μm for CS2003 at 50°C) the final and maximum distances are equal within the measurement

error, indicating a purely viscous response. In this range the speed of the translation is about 100μm/s for the Cs2003 and about 20μm/s for 8CB. The large difference between the speeds and the viscoelastic parameters of CS2003 and 8CB seen in Figure 4 is due not only to the differences in temperature but also to the shorter defect lines observed in the SmC phase of CS2003. Another difference between the studied materials is that the bookshelf layer structure is stable in CS2003, whereas in *8CB* the layers reorient in strong electric fields. During the layer transformations (2.5V/μm <E< 4V/μm) defects are generated resulting in a decrease of the speed and of the viscoelastic parameter *Γ*. At higher fields (E> 4V/μm), the alignment becomes uniformly homeotropic and Γ reaches 1 again indicating viscous response (see Figure 4(b)). Although we do not yet have a quantitative model for the physical mechanism of the rotation – triggered translational motion, we can estimate the magnitude of the viscosity by comparing the speed measured in the smectic phase to that measured in the nematic phase, where the flow viscosity values are already known for 8CB.[20] In the nematic phase at 35°C and at 3V/μm field we measured v=250μm/s, which is about 20 times larger than that measured in the smectic A phase (see Figure 4 (b)). The translational motion mainly involves flow with the director being parallel to the shear plane and normal to the velocity (η_c). From the published[20] value of η_c=0.09Pas we therefore get η_c~1.8Pas in the SmA phase at 32°C. This is of the same order as η_a estimated from the electro-rotation experiment, indicating the feasibility of using the field induced motion of particles to characterize the rheological properties in the smectic phases.

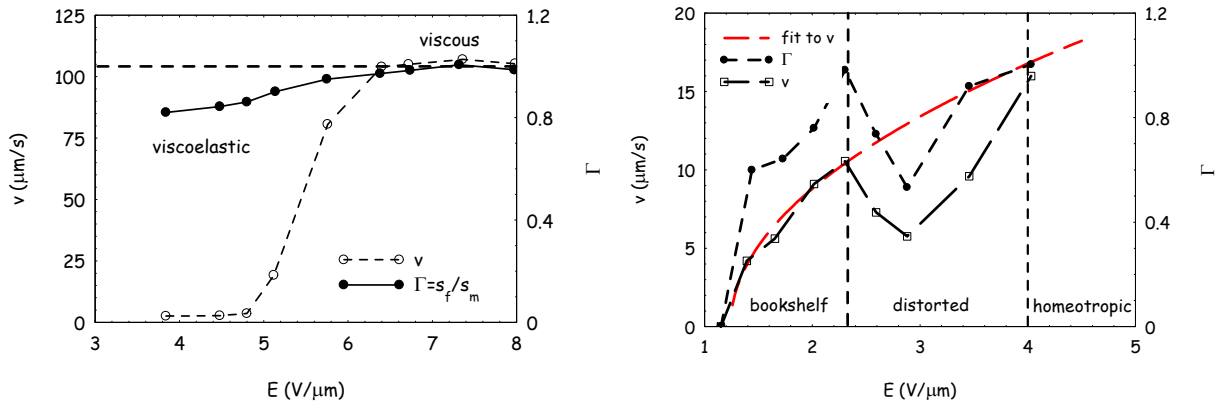

Figure 4: The speed v and the viscoelastic parameter Γ of the liquid crystals probed by the motion of 4.5μm diameter spherical glass particles as the function of the amplitude of the 1s long electric pulses. (a) CS2003 in the SmC phase at T=50°C; (b) 8CB in the SmA phase at T=32°C.*

In the films where the homeotropic texture remains stable after field removal, similar to the bookshelf alignment, defect lines form at zero field, but now they span vertically normal to the cell substrates (see *Figure 5*(a-c)). In addition, some of the particles, that were originally close to a substrate (*Figure 5*(a)), gradually (in about 10 minutes) move toward the center of the cell (*Figure 5*(b)) probably because the spheres at the surfaces lead to inclined smectic layers which cost surface anchoring energy.[21] When we apply electric fields in the horizontal layer alignment, the vertical defect lines gradually disappear just as in the bookshelf alignment (see *Figure 5*(d-g)).

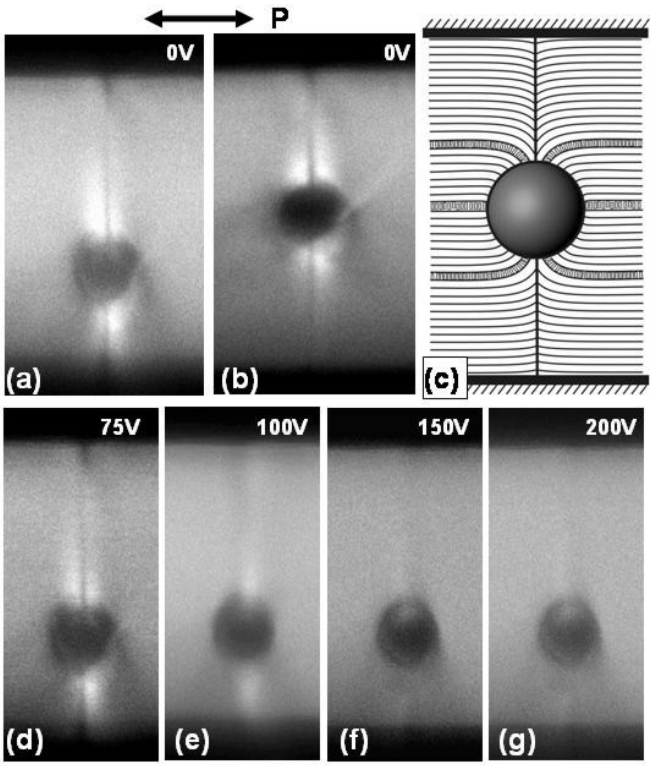

Figure 5: Vertical FCPM textures of 8CB at room temperature in horizontal layer alignment. (a,b): Textures around 4.5μm glass bead right after the field has been turned off (a) and 10 minutes later (b); (c): The corresponding layer pattern around a sphere. The director structure has rotational symmetry around the vertical defect lines. (d-g). Textures around a bead under different electric fields: 3V/μm (d), 4V/μm (e), 6V/μm (f) and 8V/μm (g).

In summary, we have presented the first observations of DC electric-field-induced rotational and translational motion of finite particles in liquid crystals. We showed that the electric field – induced rotation is analogous to the Quincke rotation, and its proper analysis can be used to measure the viscosity coefficient η_a of smectic liquid crystals. This is especially important, because this method does not require uniform alignment over centimeter ranges, and allows one to probe local viscous properties. We also demonstrated that the electro-rotation triggers a translational motion along the smectic layers. The details of the physical mechanism of the field – induced translational motion, and the defect disappearance mechanism will be subject of future studies.

Acknowledgement: Part of this work was financially supported by NSF, Grant DMR-0315523.

References:

[1] "Interfacial Electrokinetics and Electrophoresis", Ed. Á.V. Delgado, Marcel Dekker, Inc., New York (2002)
[2] W. Weiler, Z. Phys. Chem. Unterricht, Heft IV, 194 (A) (1893)

[3] G. Quincke, *Ann. Phys. Chem.,* **11**, 27 (1896)
[4] T.B. Jones, *IEEE Trans. IAS* **1A-20**, 845 (1984), and in "Electromechanics of Particles", Cambridge Univ. Press., New York, (1995)
[5] Y. Solomentsev, J.L. Anderson, *J. Fluid. Mech.,* **279**, 197-215 (1994)
[6] D. Long, A. Ajdari, *Phys. Rev. Lett.*, **81**, 1529 (1998)
[7] D. Mizumo, Y. Kimura, R. Hayakawa, *Phys. Rev. Lett.,* **87**, 088104-1 (2001) and *Phys. Rev. E*, **70**, 011509 (2004)
[8] For a review see T. Gisler, D. A. Weitz, *Curr. Opin. Colloid & Interface Sci.*, **3**, 586 (1998); F.C. MacKintosh, C.F. Schmidt, *ibid*., **4**, 300 (1999)
[9] A. Palmer, T.G. Mason, J. Xu, S.C. Kuo, D. Wirtz, *Biophys. J.,* **76**, 1063 (1999)
[10] R.G. Horn, M. Kleman, *Ann. Phys. (Paris)*, **3**, 229 (1978); S. Battacharya, S.V. Letcher, *Phys. Rev. Lett.* **44**, 414 (1980)
[11] R. G. Larson, "The structure and rheology of complex fluids", Oxford university Press, 1999
[12] N.A. Clark, *Phys. Rev. Lett.*, **40**, 1663 (1978)
[13] H.G. Walton, I.W. Stewart, M.J. Towler, *Liq. Cryst.,* **20**, 665 (1996); M.J. Towler, D.C. Ulrich, I.W. Stewart, H.G. Walton, P. Gass, *Liq. Cryst.,* **27**, 75 (2000)
[14] I. I. Smalyukh, S. V. Shiyanovskii, and O. D. Lavrentovich, *Chem. Phys. Lett.,* **336**, 88 (2001)
[15]M. Kleman and O.D. Lavrentovich, *Soft Matter Physics: An Introduction*, Springer, New York, 638 pp (2003)
[16] J.Q. Feng, *Journal of Colloid and Interface Science,* **246**, 112-121 (2002)
[17] S. Krause, P. Chandratreya, *Journal of Colloid and Interface Science*, **206**, 10 (1998)
[18] P. Panizza, P. Archambault, D. Roux, *J. Phys. II France,* **5**, 303 (1995)
[19] C. Blanc and M. Kleman, *Eur. Phys. J. E,* **4**, 241 (2001)
[20] H. Kneppe, F. Schneider, N.K. Sharma, *J. Chem. Phys.,* **77**, 3203 (1982)
[21] Z. Li and O. Lavrentovich, *Phys. Rev. Lett.,* **73,** 280 (1994)